Power Quality Enhancement of Smart Households Using a Multilevel-THSeAF With a PR Controller

Alireza Javadi, *Student Member, IEEE*, Abdelhamid Hamadi, Auguste Ndtoungou, and Kamal Al-Haddad, *Fellow, IEEE*

***Abstract*—In this paper a multilevel transformerless hybrid series active filter is proposed to enhance the power quality of a single-phase residential household. The proposed topology reflects new trends of consumers toward electronic polluting loads and integration of renewable sources which in fact may lead to the scope of a reliable and sustainable supply. This paper contributes to improvement of power quality for a modern single-phase system and emphasis integration of a compensator with energy storage capacity to ensure a sustainable supply. A proportional resonant (P+R) regulator is implemented in the controller to prevent current harmonic distortions of various non-linear loads to flow into the utility. The main significant features of the proposed topology include the great capability to correct the power factor as well as cleaning the grid simultaneously, while protecting consumers from voltage disturbances, sags, and swells during a grid perturbation. It investigates aspects of harmonic compensation and assesses the influence of the controller's choice and time delay during a real-time implementation. Combinations of analysis and experimental results performed on a laboratory setup are presented for validation.**

***Index Terms*—Hybrid active filters, power quality, renewable energy sources, multilevel converters, smart grids, real-time control, resonant controller, nonlinear loads.**

I. Introduction

THE TRENDS toward a future Smart Grid implementation and the ever increase of numerous nonlinear industrial, commercial and residential type of loads that are generating pollution which led to 100% of total current harmonic distortions into the grids have drastically created a concern on power quality metrics for future power systems [1].

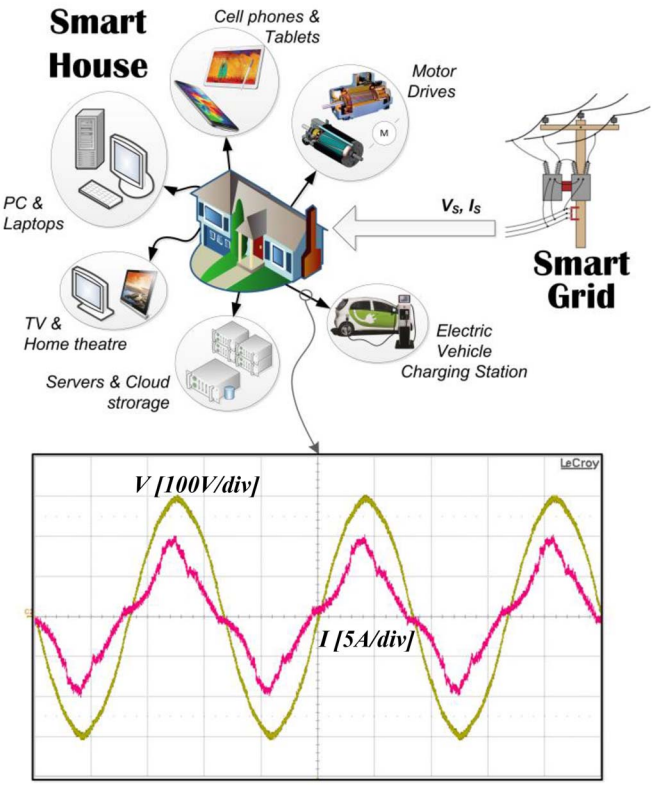

Fig. 1. Typical modern residential consumer with non-linear electronic loads and a Nissan LEAF measured voltage and current waveforms plugged to a level-2 charging station.

The increase in electronics devices as shown in Fig. 1, associated with fast charging [2], [3] devices with external energy sources require early investigation on harmonic and non-active power compensation [4]. This widespread harmonic polluting device not only reduce the system's efficiency, but also has detrimental impacts on grid voltage distortion levels [5]. Likewise, distorted current waveform creates additional heating losses, and causes failure in sensitive electrical devices. Several references could be found in the literature addressing specified [6], [7] or common cases dealt with power quality issues either related to voltage distortions or current harmonics [8].

This paper addresses the new research challenges that are facing the power electronics converters to participate actively

Manuscript received September 25, 2015; revised April 7, 2016 and July 11, 2016; accepted August 22, 2016. Date of publication September 12, 2016; date of current version December 21, 2016. This work was supported in part by the Natural Sciences and Engineering Research Council of Canada-CRSNG, in part by the Canada Research Chair in Electrical Energy Conversion and Power Electronics, and in part by the CRC-EECPE of Montreal. Paper no. TSG-01189-2015.

A. Javadi, A. Hamadi, and A. Ndtoungou are with the Electrical Engineering Department, École de Technologie Supérieure, University of Quebec, Montreal, QC H3C1K3, Canada (e-mail: alireza.javadi.1@ens.etsmtl.ca).

K. Al-Haddad is with the CRC-EECPE, École de Technologie Supérieure, University of Quebec, Montreal, QC H3C1K3, Canada (e-mail: kamal.al-haddad@etsmtl.ca).

Color versions of one or more of the figures in this paper are available online at http://ieeexplore.ieee.org.

Digital Object Identifier 10.1109/TSG.2016.2608352

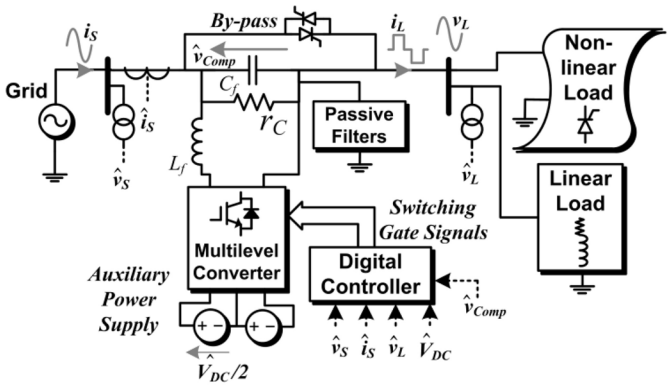

Fig. 2. House equivalent circuit connection with utility meters and the Multilevel-THSeAF connected in series.

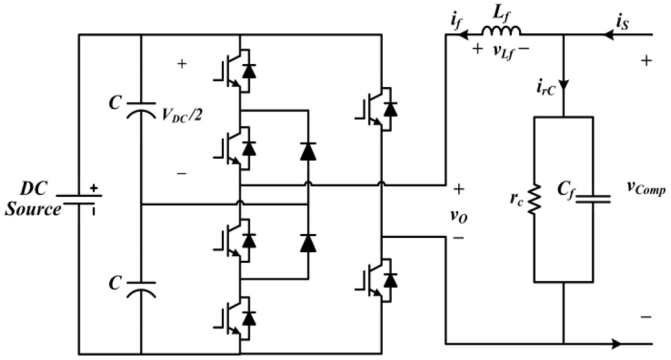

Fig. 3. Hybrid converter topology for the proposed series compensator.

TABLE I
CONFIGURATION PARAMETERS

Symbol	Definition	Value
V_S	Line phase-to-neutral voltage	110 Vrms
f	System frequency	60 Hz
L_S	Supply equivalent inductance	150 μH*
R, L	Non-linear CSC load	25 Ω, 20mH
Lf	Switching ripple filter inductance	2.5 mH
Cf	Switching ripple filter capacitance	2 μF
r_C	Switching ripple damping resistor	60 Ω
Ts	Opal-RT Synchronous sampling time	40 μs
f_{PWM}	PWM frequency	8 kHz
F_5	Fifth order shunt passive filter	56μF, 5mH
F_7	Seventh order passive filter	14μF, 10mH
F_{11}	Eleventh order passive filter	6μF, 10mH
F_{HPF}	High-pass filter	2μF
K_P, K_r	Controller proportional and resonant gains	2.5, 10
ω_C	Cutoff frequency	5 rad/s
V_{DC}	dc auxiliary power supply voltage	110 V, 120 V*

* Adopted value for the simulation analysis

in mitigating electric types of pollution and consequently enhance the grid so as to supply clean and reliable energy to the fast-growing energy demand [9] by highly nonlinear and time varying loads. The efficient and affordable solution proposed in this paper uses a multilevel configuration [10] to reduce dc side voltage for low level distribution system as demonstrated in Fig. 2. The use of this device will facilitate the integration of energy storage systems and renewables for modern households [11], [12]. It is noteworthy to mention that this proposed configuration does not necessitate the bulky series transformer [13] which constitute an economic key toward cost effective power quality improvement of future grids.

This multifunctional compensator cleans the current drawn from the utility and similarly to a Dynamic voltage restorer (DVR) the point of common coupling (PCC) and utility smart meters will be protected from voltage distortions so as to avoid wrong computation of power and energy balance. This compensator could inject or absorb active power during grid voltage variations to ensure high quality supply along with complete decoupling from polluted loads.

The increase of charging stations [14] in a residential neighborhood and commercial buildings becomes crucial to monitor and evaluates their power quality characteristics [15]. In addition, pushed by social efforts, distributed generation and renewable energy sources are been popularized requiring more research and investigation on their wide application on the power quality of the system [16]. This work proposes an efficient Transformerless Hybrid Series Active Filter (THSeAF) capable of rectifying current related issues in such microgrid application and provides sustainable and reliable voltage supply at the PCC where important residential consumers are connected.

This paper is organized as follows; the system configuration will be first introduced. Then the operation principle of the proposed configuration is explained. The third section will be dedicated to the modeling and analysis of the control algorithm. The voltage and current harmonic detection method is explicitly described. To evaluate the proposed topology and control behavior, several scenarios are simulated and experimental validations will be presented and discussed.

II. SYSTEM ARCHITECTURE

A. System Configuration

The compensator depicted in Fig. 2 is composed of a multilevel single-phase converter connected in series between the utility and the house's entrance connected terminals. The transformerless hybrid series active filter is composed of a five-level NPC converter [17] depicted in Fig. 3, connected in series between the utility and the entrance of the building. An auxiliary supply is connected on the dc side. To filter high frequency switching harmonics, a passive filter is used at the output of the converter. A bank of tuned passive filters ensures a low impedance path for current harmonics. In this paper the studied system is implemented for a rated power of 1 kVA. To ensure a fast transient response with sufficient stability margins over a wide range of dynamic operations, the controller is implemented on an Opal-RT/Wanda real-time simulator. For an accurate real-time measurement of electrical variables, the Opal-RT OP8665 probes are performing the measurement task. The system parameters are identified in Table I. A variable source up to 120 Vrms is connected to

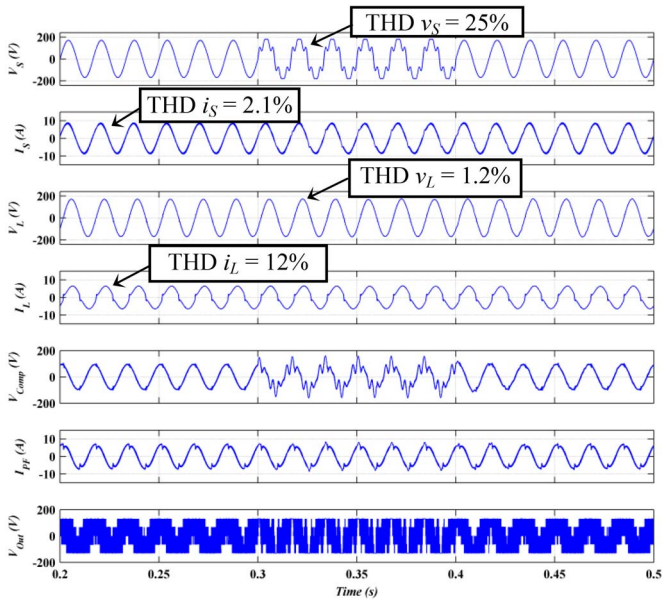

Fig. 4. Compensating current harmonics and voltage regulation, during grid initiated distortions. (a) Source voltage v_S, (b) source current i_S, (c) load voltage v_L, (d) load current i_L, (e) active-filter voltage V_{Comp}, (f) Harmonics current of the passive filter i_{PF}, (g) Converter's output voltage V_{Out}.

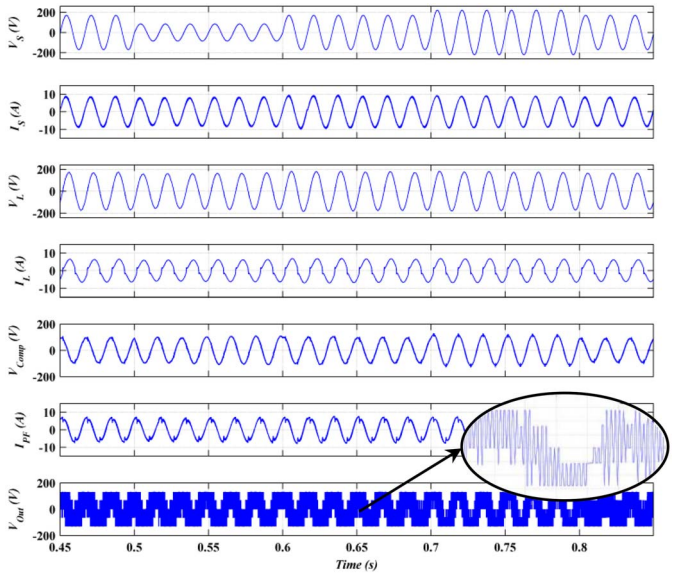

Fig. 5. System response during grid sags and swells. (a) Source voltage v_S, (b) source current i_S, (c) load voltage v_L, (d) load current i_L, (e) active-filter voltage V_{Comp}, (f) Harmonics current of the passive filter i_{PF}, (g) Converter's output voltage V_{Out}.

a 1 kVA non-linear load. The THSeAF is connected in series in order to inject the compensating voltage. On the DC side of the compensator, an auxiliary dc-link energy storage system is installed. Similar parameters are also applied for simulations. A fast electric vehicle charging plug level-2 is as well connected to the load's PCC. The active compensator's NPC converter structure is depicted in Fig. 3.

On the DC side of the compensator, auxiliary dc-link energy storage components are installed at a reduced voltage level of 100V. The objective is to propose an efficient device capable of rectifying current related issues in smart grids which also provide sustainable and reliable voltage supply at the point of common coupling that define the entrance of residential or commercial buildings.

Using the circuit of Fig. 2 showing the block diagram and model of equivalent house circuit connection with utility meters and Multilevel-THSeAF connected in series, several critical scenarios such as grid distortion, sag or swell are simulated using discrete time steps of 40μs as shown in Fig. 4 and Fig. 5. The Multilevel-THSeAF connected in series injects a compensating voltage which results in a drastic improvement of source current distortions and a cleaned load voltage. While the load current contains a THDI_L of 12%, the source current is cleaned with a THDI_S of 2.1%. When the utility is highly polluted with a THDV_S of 25.5%, the load voltage is regulated and contains a THD of only 1.2%.

B. Operation Principle

A current fed type of non-linear load could be modeled as a harmonic voltage source in series with an impedance $Z_{Non-Linear}$ or by its Norton equivalent modeled with a harmonic current source in parallel to the impedance. Thévenin's model and Norton's equivalent circuit are depicted in Fig. 6. In this paper the common Norton's equivalent is chosen to follow major related papers. In this work the approach to achieve optimal behavior during the time the grid is perturbed is implemented on the controller [18]. The use of a passive filter is mandatory to compensate current issues and maintaining a constant voltage free of distortions at the load terminals. The non-linear load is modeled by a resistance representing the active power consumed and a current source generating harmonic current. Accordingly, the impedance Z_L is the equivalent of the nonlinear ($Z_{Non-linear}$) and the linear load (Z_{RL}). The Series active filter, whose output voltage V_{comp} is considered as an ideal controlled voltage source is generating a voltage based on the detecting source current, load voltage, and also the source voltage to achieve optimal results as of (4). This established hybrid approach gives good result and is quite less sensitive to the value of the gain $\boldsymbol{G}$ to achieve low levels of current harmonics. The gain $\boldsymbol{G}$ is proportional to the current harmonics (I_{sh}) flowing to the grid. Assuming a non-ideal grid supplying feeder voltage that contains important numbers of voltage distortions (V_{Sh}), the equivalent circuit for the fundamental and harmonics are:

$$V_S = V_{s1} + V_{sh} \tag{1}$$

$$V_L = V_{L1} + V_{Lh} = Z_L I_Z = Z_L(I_S - I_h) \tag{2}$$

$$I_S = I_{S1} + I_{Sh} = I_Z + I_h \tag{3}$$

$$V_{Comp} = +GI_{Sh} - V_{Lh} + V_{Sh} \tag{4}$$

Where I_Z represents the load current in Z_L shown in Fig. 6. Using the Kirchhoff's law the following equation is depicted for both the fundamental and harmonics.

$$V_S = Z_S I_S + V_{Comp} + V_L \tag{5}$$

$$V_{L1} = Z_L I_{S1}, \quad V_{Lh} = Z_L(I_{Sh} - I_h) \tag{6}$$

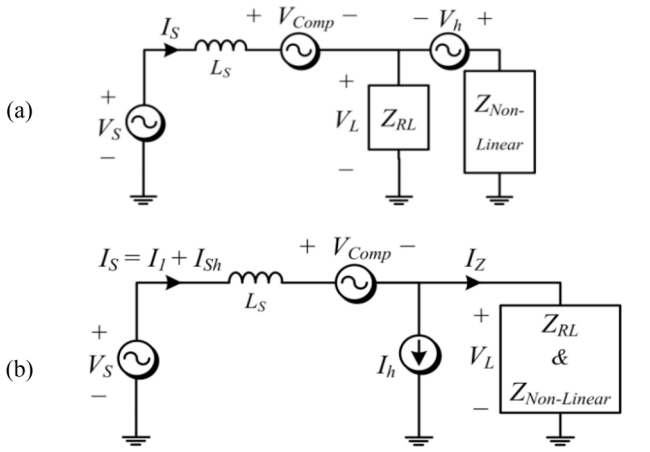

Fig. 6. Single-phase equivalent phasor model for VSC type of loads, (a) Thévenin's model, (b) Norton equivalent.

By substituting the fundamental of (6) in (5), the source current at fundamental frequency is obtained.

$$I_{S1} = \frac{V_{S1}}{Z_S + Z_L} \tag{7}$$

By substituting (4) in (5) for the harmonic components, the harmonic source current is reached as follow.

$$V_{Sh} = Z_S I_{Sh} + G I_{Sh} - V_{Lh} + V_{Sh} + V_{Lh} \rightarrow I_{Sh} = 0 \tag{8}$$

By introducing (8) into the harmonic component of the load PCC voltage (6), following equation is achieved.

$$V_{Lh} = -Z_L I_h \tag{9}$$

Consequently in this approach even in presence of source voltage distortions the source current is always clean of any harmonic component. To some extent in this approach the filter behaves as high impedance likewise an open circuit for current harmonics, while the shunt high pass filter tuned at the system frequency, could create a low-impedance path for all harmonics and open circuit for the fundamental component. This argument explains the need of a Hybrid configuration to create an alternative path for current harmonics fed from a current source type of nonlinear loads.

III. Modeling and Control of the Single-Phase Multilevel-THSeAF

A Transformerless Hybrid series active filter configuration is considered in this paper in order to avoid current harmonic pollution along the power line caused by a single-phase diode bridge rectifier load, followed by an inductor L_{NL} in series with a resistor R_{NL}. The sequences of the modulation are presented in Fig. 7.

A. Modeling of Transformerless Series Active Filter

According to Fig. 3, and the average equivalent circuit of an inverter developed in [19], the small-signal model of the proposed configuration can be obtained. Kirchhoff's rules for voltages and currents, as applied to this system, provide us with the differential equations.

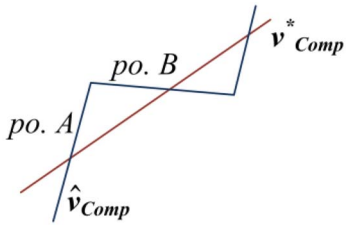

Fig. 7. Compensating voltage versus the reference signal.

Thereafter, d is the duty cycle of the upper switch of the converter leg in a switching period, whereas $\bar{v}$ and $\bar{\imath}$ denotes the average value in a switching period of the voltage and current of the same leg. The mean converter output voltage and current are expressed by (10) and (11) as follows.

$$\bar{v}_O = \left(\underbrace{2d-1}_{m}\right) V_{DC} \tag{10}$$

$$\bar{\imath}_{DC} = m\bar{\imath}_f \tag{11}$$

According to the scheme on Fig. 3, the arbitrary direction of i_f is chosen to go out from the H-bridge converter. For dynamic studies the accurate model is considered.

$$mV_{DC} = L_f \frac{di_f}{dt} + v_{Comp} \tag{12}$$

$$r_C C_f \frac{dv_{Comp}}{dt} = -v_{Comp} + r_C\left(i_f + i_S\right) \tag{13}$$

The state-space small-signal ac model could be derived by a linearized perturbation of averaged model as follow:

$$\dot{x} = Ax + Bu \tag{14}$$

Hence we obtain:

$$\frac{d}{dt}\begin{bmatrix} \bar{\imath}_f \\ \bar{v}_{Comp} \end{bmatrix} = \begin{bmatrix} 0 & -\dfrac{1}{L_f} \\ \dfrac{1}{C_f} & -\dfrac{1}{r_C C_f} \end{bmatrix} \times \begin{bmatrix} \bar{\imath}_f \\ \bar{v}_{Comp} \end{bmatrix} + \begin{bmatrix} \dfrac{V_{DC}}{L_f} & 0 \\ 0 & \dfrac{1}{C_f} \end{bmatrix} \times \begin{bmatrix} m \\ i_S \end{bmatrix}. \tag{15}$$

The output vector is then:

$$y = Cx + Du \tag{16}$$

or

$$y = \begin{bmatrix} 0 & 1 \end{bmatrix} \times \begin{bmatrix} \bar{\imath}_f \\ \bar{v}_{Comp} \end{bmatrix} \tag{17}$$

By means of (15) and (17), the state-space representation of the model could be obtained.

The second order relation between the compensating voltage and the duty cycle could be reached as follows.

$$C_f \frac{d^2 v_{Comp}}{dt^2} + \frac{1}{r_C}\frac{dv_{Comp}}{dt} + \frac{1}{L_f} v_{Comp} = \frac{V_{DC}}{L_f} m + \frac{di_S}{dt} \tag{18}$$

This model could then be used in developing the converter's controller and its stability analysis.

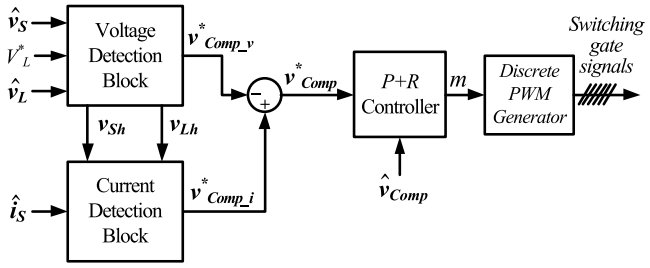

Fig. 8. Control system architecture scheme for P+R.

IV. Control Algorithm of the System

The Multilevel Transformerless Hybrid series active filter configuration considered in this work is taking advantage of an NPC converter to reduce passive components rating while, delivering a high-quality compensating voltage. The controller strategy implemented in this paper is based on a Proportional plus resonant controller to generate IGBT's gate signals. The reference signal applied to the P+R regulator is created by two detection block taking care of the voltage and current issues respectively as presented in the following control diagram.

In this Rapid Control Prototyping (RCP) application, the whole controller is implemented on the Opal-RT device, where the controller is run on a fixed time step size determined in the core of the paper in Table I. The inputs of the controller described in Fig. 8, are measured using the Opal-RT probes. The output signals of the controller are the switching gate signals produced over the digital output of the real-time simulator. These signals are then passing through opto-isolator board to enable semiconductor gate driver's control.

As the compensating voltage reference is an oscillating signal with several harmonic components, the P+R regulator has numerous advantages over other control approaches. To develop the controller, the average equivalent circuit of the converter is used with the small-signal model of the proposed configuration to analyze the effects of delays on the transient response of the compensator. The proposed control strategy takes advantages of both a proportional and resonant controller to generate gating signals.

The transfer function of the controller with a multi-resonant property is given by:

$$G_{P-R}(s) = K_P + \sum_{h=1,3,5,7,\ldots}^{n} \frac{2K_{rh} \cdot \omega_C \cdot s}{s^2 + 2\omega_C \cdot s + (h \cdot \omega)^2} \tag{19}$$

Where h is the harmonic order, K_p and K_{rh} are gains, and $h\omega$ is the resonant frequency and ω_C is the cutoff frequency. Their values are depicted in Table I. The frequency responses with a delay time are depicted in Fig. 9, where the Bode diagram shows the superiority of the PR controller over the system without regulation and with a PI regulator.

To implement the controller on the digital simulator the transfer function should be obtained by discretization via numerical integration. To obtain the discrete equivalent of a transfer function via numerical integration, one should apply appropriate numerical integration techniques depending on the sensitivity and stability requirements to the system differential equation [20].

The P+R controller function is then calculated, where z is the variable in the z-domain and T is the sampling time constant also known as step-time T_S in Matlab environment.

By performing the Z-transform, using the Tustin or bilinear approximation based on e trapezoidal rule, on (19), the discrete transfer function is achieved as follow. The frequency variable "s" is replaced by the following term.

$$s \to \frac{2 \cdot (z-1)}{T(z+1)}, \quad s^2 \to \frac{4(z-1)^2}{T^2(z+1)} \tag{20}$$

This results in the following discrete transfer function in the z-domain.

$$G_{P+R}(z) = K_P + \sum_{h=1,3,5,7,\ldots}^{n} \frac{2K_{rh} \cdot \omega_C \cdot z^2 \cdot T - K_{rh} \cdot \omega_C \cdot T}{(1 + \omega_C T + (h\omega T)^2)z^2 + \left(\frac{(h\omega T)^2}{2} - 2\right)z + 1 - \omega_C T + \frac{(h\omega T)^2}{4}} \tag{21}$$

According to the two developed discrete function, one can implement either of them for a real-time simulation or a practical experiment on a digital controller. Meanwhile, the choice of gains is tied with the stability study of the transfer function. The gains should be chosen depending on the sampling time imposed by the digital controller, and the behavior of the system itself. In a general rule; the more the sampling time T, has a smaller value, the more the chance to reach a stable system is observed.

V. Steady State Power Flow of Active Series Compensation

As apprehended earlier, the series compensator behaves as a controllable voltage source generating waveforms having harmonic components up to the tuned allowable limits imposed by the designer based on parameters of the compensator, in this work 8 kHz is chosen to remain in the stable operating point. In this section the equivalent circuit of the standalone active compensator without the shunt passive filter as shown in Fig. 10 is taken into account. The load flow is performed for the steady state condition and assumes a lagging load. It is noteworthy to mention the three following principles to remember for the series compensation:

- The series source does not inject or absorb current. This lead to the fact that the load current and source current are identical. As the duality of a shunt active filter, here the line current passes directly through the series compensator ($I_S = I_L$);
- The load flow is performed at the fundamental frequency, and thus the harmonics are not considered in this study ($I_h = 0$);
- In a general form, it is impossible to control the DC bus voltage of the compensator and correcting the power factor simultaneously as both are using one single variable, the phase angle.

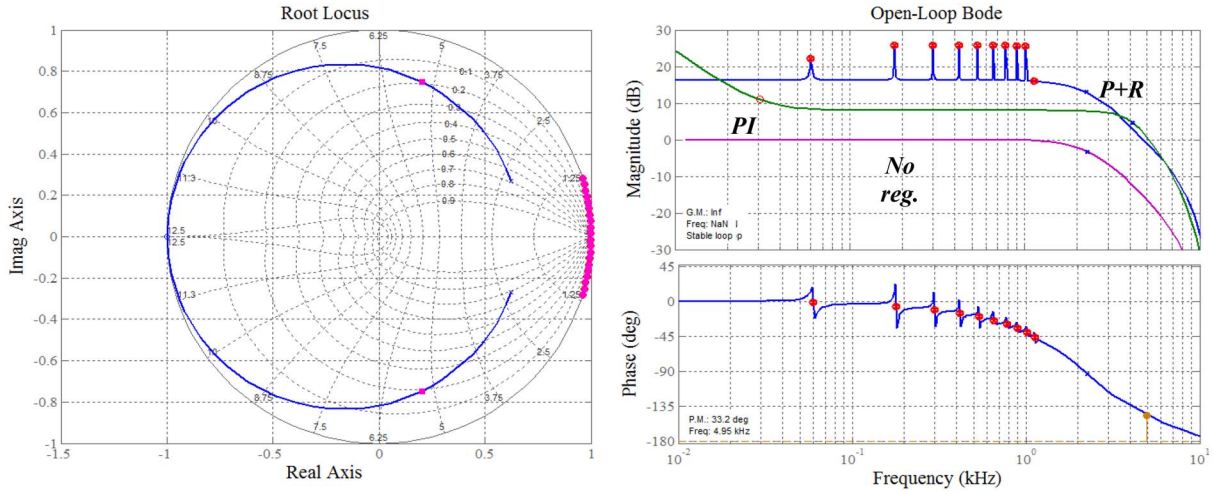

Fig. 9. Frequency response of the system with a 40 μs delay time; using the PI controller, P+R controller, and with a closed-loop controller. (a) Root Locus diagram. (b) Bode diagram.

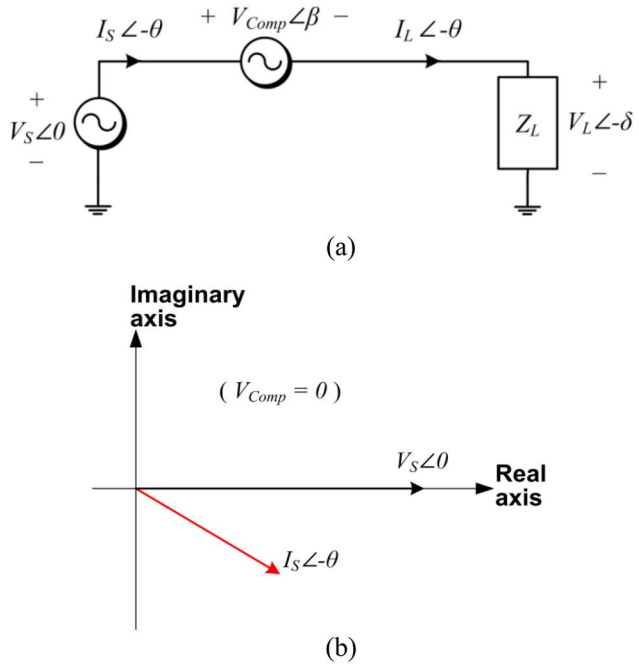

Fig. 10. (a) Circuit diagram of a radial system with the series active compensator, (b) Phasor diagram of the radial system before compensation with VS as reference.

For sake of simplicity, the load voltage amplitude is considered equal to the source voltage rms value.

A. Power Factor Compensation

The polar representation of the system becomes as of Fig. 11, where line current and source voltage are in phase. The power flow for each component of the radial circuit for the inductive load could be found. By shifting the load voltage, the compensator forces the load to drift a current which will be in-phase with the source voltage respectfully.

In a general form, the auxiliary dc supply should be designed according to the maximum compensating voltage that the compensator is tasked to provide at the fundamental

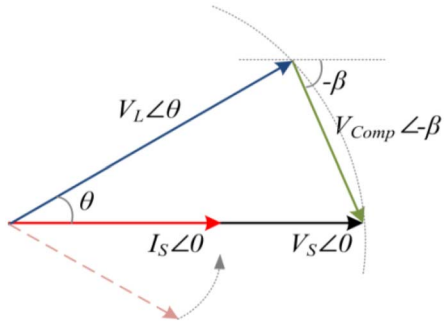

Fig. 11. Phasor diagram while correcting the power factor.

frequency. The DC bus voltage could not be lower than the maximum value of the compensation voltage at fundamental.

$$V_{DC} \geq V_{Comp\_max} \Rightarrow 0 \leq \left|V_{Comp}\right| \leq V_{DC} \tag{22}$$

The compensator rating will be equal to the percentage of the produced compensation voltage. Thus, the rating of the SeAF could vary from around 30% of the load power up to the full load. The rated power to design the compensator could be calculated as follows.

$$S_{SeAF} = V_{Comp} I_L \; \left(I_{Comp} = I_S = I_L\right) \tag{23}$$

Back to the previous vector representation the angle of the produced compensating voltage could be calculated as follows:

$$\beta = \frac{180 - \theta}{2} \tag{24}$$

By assuming that $|V_L|$ is equal to $|V_S|$, the complex apparent power which is the product of the voltage and the conjugate of the current could be calculated as follows. The power supplied by the grid is:

$$S_S = (V_S \angle 0)(I_S \angle 0)^* = |V_S||I_S| \angle 0 = P_S \tag{25}$$

The amount of power consumed by the load is:

$$S_L = (V_L \angle \theta)(I_L \angle 0)^* = |V_S||I_S| \angle \theta = P_L + jQ_L \tag{26}$$

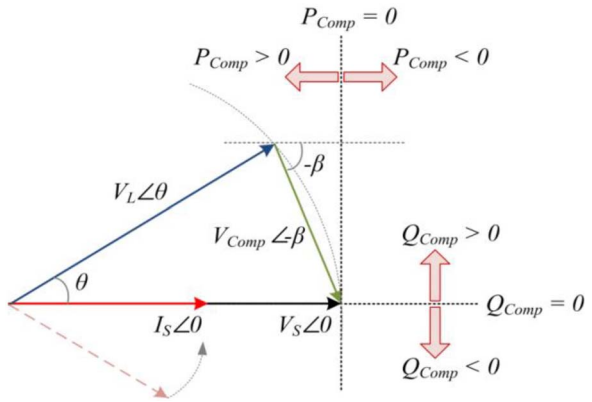

Fig. 12. Phasor diagram and compensator's power representation.

The amount of power supplied by the compensator is:

$$S_{Comp} = \left(V_{Comp}\angle - \beta\right)(I_S\angle 0)^* = \left|V_{Comp}\right|\left|I_{Sh}\right|\angle - \beta = P_{Comp} - jQ_{Comp} \tag{27}$$

With regards to calculated powers, it is obvious that the source supplies only active power, while the load continues to consume the same active and reactive power as before. The compensator is absorbing the arithmetical difference of active powers between the source and load and supplies the difference of reactive power again between the source and the load.

$$\begin{cases} P_{Comp} = P_S - P_L \\ Q_{Comp} = -Q_L \end{cases} \tag{28}$$

The direction of the power flow for the compensator has arbitrarily been chosen as follows: if the compensator absorbs the power it has a positive value and if it injects or supply power, the power will have a negative value.

It is noteworthy to mention that, if the source voltage amplitude is equal to the load's voltage, the compensator will absorb power, while if the load voltage is much greater than the source one, then the compensator starts to supply active power as illustrated in Fig. 12. Likewise for the reactive power; if the load has a lagging power factor, the compensator will supply reactive power and if the load has a leading power factor (capacitive load) the compensator will absorb the desired amount of reactive power to finally achieve a unity PF.

The following result shows a series compensator (a DVR) correcting the power factor. A UPF is reached even during a dynamic change in the load power. The DVR has shifted the load's voltage by applying a compensating voltage at fundamental frequency where its vector representation is illustrated in Fig. 12.

By sweeping the load voltage, the load current will follow in the same direction as shown in Fig. 13. As a consequence the line current become in phase with the grid voltage resulting in a unity PF. The compensator will keep the PF at unity value even when the load has increased at 0.2s by supplying more reactive power. The calculated powers in Fig. 14 illustrate the amount of active and reactive powers flow in each section and show the exceeding amount of power absorbed or injected by the auxiliary DC source. As soon as the Series compensator

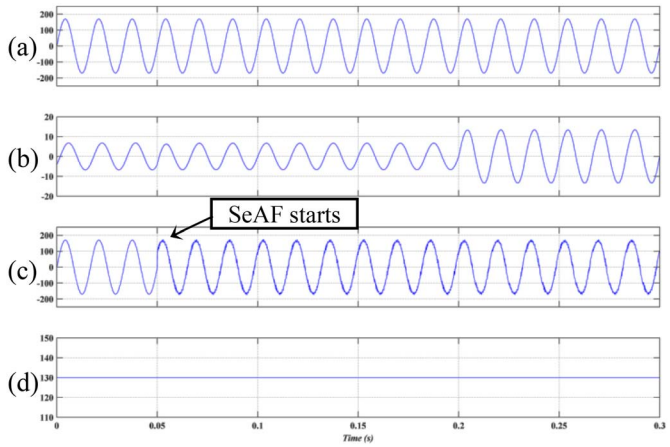

Fig. 13. Series compensator to correct the power factor; (a) Grid voltage v_S, (b) source current i_S, (c) load voltage v_L, (d) DC bus voltage V_{DC}.

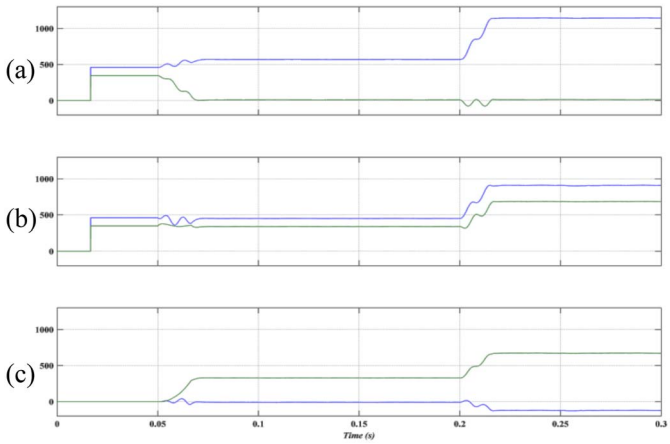

Fig. 14. Series compensator with DC source correcting the power factor, calculated powers; Active power (blue), and Reactive power (green). (a) Grid supply, (b) Load power, (c) Compensator supply.

starts operating (at 0.05s), by performing a PF correction, the reactive power exchanged by the grid drops down and is transformed to active power, while the loads power flow has not been affected. The amount of powers that each source will provide could be calculated by (25) to (28). This auxiliary source ensures a constant voltage in the DC side of the converter and the compensator's controller does not require having an integrated DC bus regulator.

VI. Experimental Results

To validate the study various scenarios similar to those effectuated in the simulation are performed on a laboratory prototype. Fig. 15 shows the setup components with parameters described in Table I. The Opal-RT real-time simulator, the NPC converter along with precise probes dedicated for RCP applications are noticeable in the picture.

The compensation during steady state depicted in Fig. 16, shows the polluted load harmonics isolated from the utility and a unity power factor (UPF) is reached. Moreover, the compensator maintains the load's voltage regulated with constant

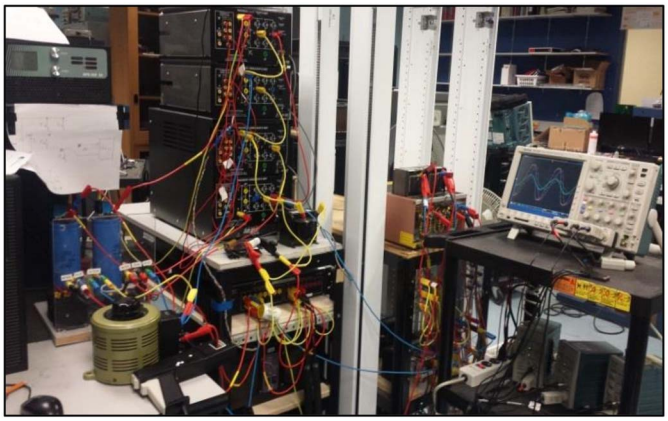

Fig. 15. Laboratory setup used for experiments.

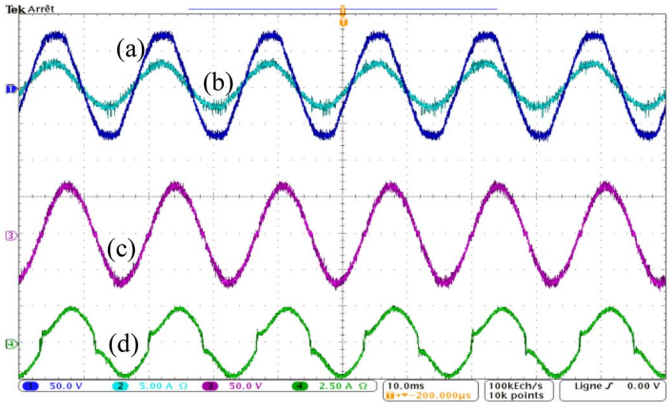

Fig. 16. Steady state waveforms of the THSeAF compensating load current. (a) Source voltage v_S [50V/div], (b) source current i_S [5A/div], (c) load PCC voltage v_L [50V/div], (d) load current i_L [2.5A/div].

amplitude and free of all kinds of distortions independently of the grid condition.

The load's voltage THD could be reduced to the desired value by performing a fine-tuning of the shunt passive filter which indirectly contributes to the voltages quality as explained in the previous section. This one-time tuning is independent of parameters of the system. The harmonic content and THD of sources and load voltage and current for the Fig. 16 are presented in Fig. 17.

The line current shows dramatic improvements in its THD while the THSeAF is operating in a hybrid approach. A gain G of 3Ω equivalent to 0.4p.u. was used to control current harmonics. As mentioned earlier, the capability of operating with reduced DC voltage is considered as one of advantage of the proposed configuration, where for these tests it is maintained at 110VDC.

Experimented results illustrate high fidelity towards simulations. During a grid's voltage sags, the compensator regulates the load voltage magnitude, compensates current harmonics and corrects the power factor as shown in Fig. 18. These figures show possible cases in which the THSeAF could face during the worst scenario requiring compensation of the load voltage harmonics.

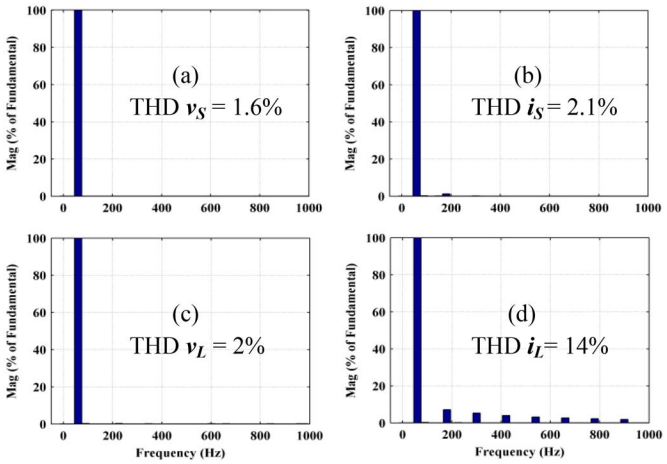

Fig. 17. Harmonic contents in percentage of fundamental when THSeAF in operation; (a, b) Source voltage and current, (c, d) Load voltage and current.

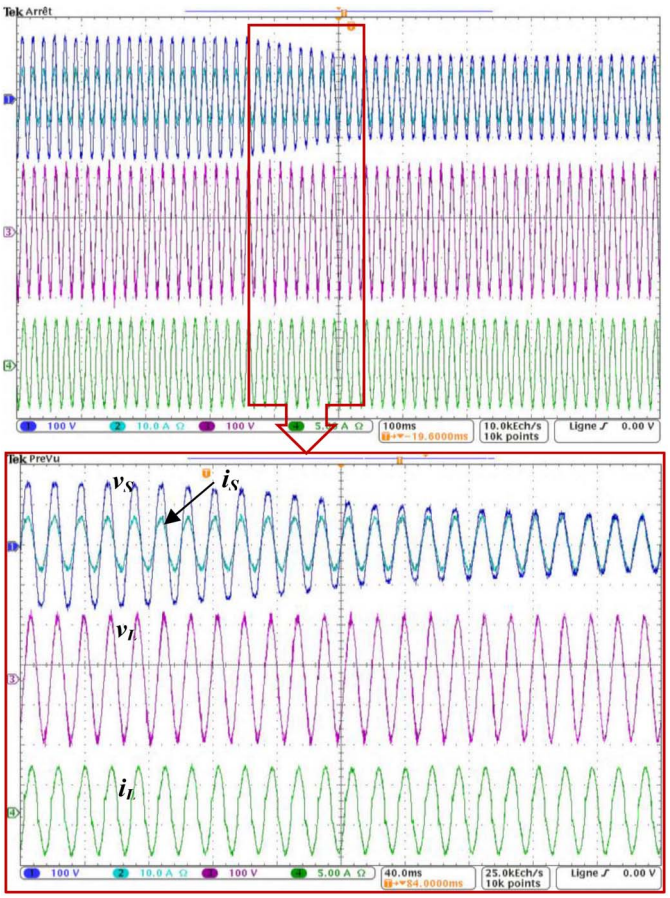

Fig. 18. Waveforms during a sags; (a) Source voltage v_S [100V/div], (b) source current i_S [10A/div], (c) load PCC voltage v_L [100V/div], (d) load current i_L [5A/div].

Clarified in Section V, the auxiliary DC source, similar to a UPS, provides necessary amount of power to maintain the supply at the load terminals despite variation in the utility's voltage magnitude. The bidirectional DC source should exchange power with an auxiliary feeder or energy storage to maintain the DC voltage at a constant value. As expected from simulations, during a grid's extended voltage swell, the

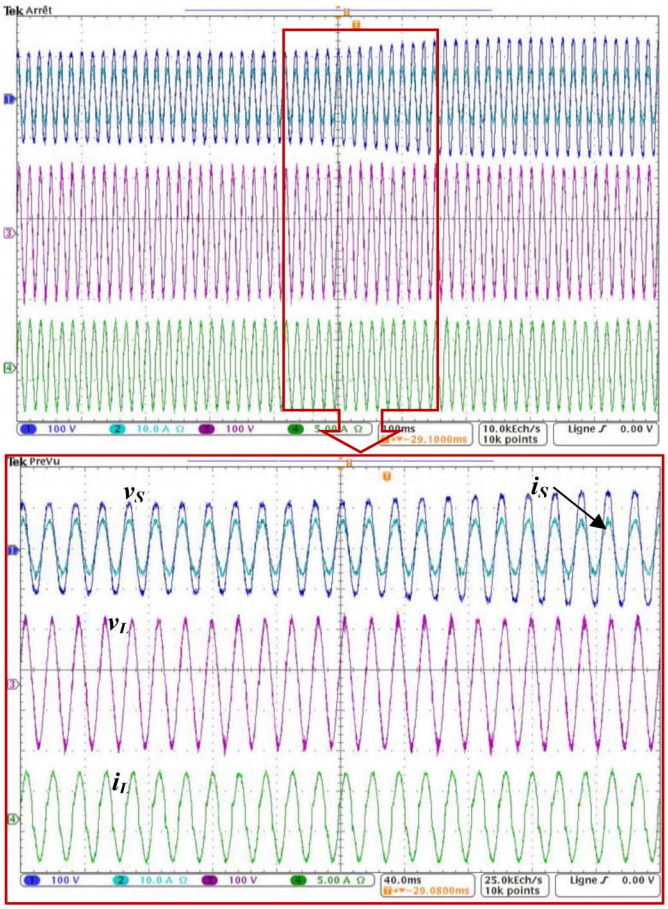

Fig. 19. Waveforms during a swells; (a) Source voltage v_S [100V/div], (b) source current i_S [10A/div], (c) load PCC voltage v_L [100V/div], (d) load current i_L [5A/div].

compensator regulates the load voltage magnitude by injecting active power while compensating current harmonics and correcting the PF as shown in Fig. 19.

VII. Summary

Renewable energy sources that are proliferating very rapidly are connected to the grid via resonant filters that may also interact with the grid impedances and can cause undesired EMI and resonance phenomenon. Therefore the necessity of maintaining clean decoupled power is becoming an important issue since electric power quality is usually measured at generation, distribution and load levels. To improve power quality, a Multilevel-THSeAF was developed in this work based on the five-level NPC configuration. The key novelty of the proposed topology includes power quality improvement in a single residential building that may result to the enhancement of the global power system. Moreover, the configuration can regulate and improve the load voltage and when connected to a renewable auxiliary DC source, the topology is able to counteract actively to the power flow in the system similar to a UPS. Having a constant and distortion-free supply at load PCC, it was denoted that the active compensator responds well to source voltage variations. Furthermore, this compensator eliminates source harmonic currents and improves grid power quality with no need to use the typical bulky series transformer. It was demonstrated that this active compensator responds properly to source voltage variations by providing a constant and distortion-free supply at load terminals. Furthermore, it eliminates source harmonic currents and improves power quality of the grid without the usual bulky and costly series transformer. The proposed transformerless configuration was simulated and experimentally validated.

References

[1] M. Liserre, T. Sauter, and J. Y. Hung, "Future energy systems: Integrating renewable energy sources into the smart power grid through industrial electronics," *IEEE Ind. Electron. Mag.*, vol. 4, no. 1, pp. 18–37, Mar. 2010.

[2] M. Yilmaz and P. T. Krein, "Review of battery charger topologies, charging power levels, and infrastructure for plug-in electric and hybrid vehicles," *IEEE Trans. Power Electron.*, vol. 28, no. 5, pp. 2151–2169, May 2013.

[3] A. Javadi, A. Ndtoungou, H. F. Blanchette, and K. Al-Haddad, "Power quality device for future household systems with fast electric vehicle charging station," in *Proc. IEEE Veh. Power Propul. Conf. (VPPC)*, Montreal, QC, Canada, 2015, pp. 1–6.

[4] J. M. Guerrero, P. C. Loh, T.-L. Lee, and M. Chandorkar, "Advanced control architectures for intelligent microgrids—Part II: Power quality, energy storage, and AC/DC microgrids," *IEEE Trans. Ind. Electron.*, vol. 60, no. 4, pp. 1263–1270, Apr. 2013.

[5] S. Zhikang *et al.*, "Series and parallel resonance problem of wideband frequency harmonic and its elimination strategy," *IEEE Trans. Power Electron.*, vol. 29, no. 4, pp. 1941–1952, Apr. 2014.

[6] H. Akagi and K. Isozaki, "A hybrid active filter for a three-phase 12-pulse diode rectifier used as the front end of a medium-voltage motor drive," *IEEE Trans. Power Electron.*, vol. 27, no. 1, pp. 69–77, Jan. 2012.

[7] A. Javadi and K. Al-Haddad, "A single-phase active device for power quality improvement of electrified transportation," *IEEE Trans. Ind. Electron.*, vol. 62, no. 5, pp. 3033–3041, May 2015.

[8] C. A. G. Marques, M. V. Ribeiro, C. A. Duque, P. F. Ribeiro, and E. A. B. Da Silva, "A controlled filtering method for estimating harmonics of off-nominal frequencies," *IEEE Trans. Smart Grid*, vol. 3, no. 1, pp. 38–49, Mar. 2012.

[9] K. Rahbar, J. Xu, and R. Zhang, "Real-time energy storage management for renewable integration in microgrid: An off-line optimization approach," *IEEE Trans. Smart Grid*, vol. 6, no. 1, pp. 124–134, Jan. 2015.

[10] E. C. D. Santos, J. H. G. Muniz, E. R. C. Da Silva, and C. B. Jacobina, "Nested multilevel topologies," *IEEE Trans. Power Electron.*, vol. 30, no. 8, pp. 4058–4068, Aug. 2015.

[11] Q. Guo, S. Xin, H. Sun, Z. Li, and B. Zhang, "Rapid-Charging navigation of electric vehicles based on real-time power systems and traffic data," *IEEE Trans. Smart Grid*, vol. 5, no. 4, pp. 1969–1979, Jul. 2014.

[12] A. Javadi, A. Hamadi, L. Woodward, and K. Al-Haddad, "Experimental investigation on a hybrid series active power compensator to improve power quality of typical households," *IEEE Trans. Ind. Electron.*, vol. 63, no. 8, pp. 4849–4859, Aug. 2016.

[13] A. Javadi, A. Hamadi, and K. Al-Haddad, "Three-phase power quality device for weak systems based on SRF and p-q theory controller," in *Proc. 41st Annu Conf. IEEE Ind. Electron. Soc. (IECON)*, Yokohama, Japan, 2015, pp. 345–350.

[14] S. Rivera, B. Wu, S. Kouro, V. Yaramasu, and J. Wang, "Electric vehicle charging station using a neutral point clamped converter with bipolar DC bus," *IEEE Trans. Ind. Electron.*, vol. 62, no. 4, pp. 1999–2009, Apr. 2015.

[15] Y. Wang, X. Lin, and M. Pedram, "Adaptive control for energy storage systems in households with photovoltaic modules," *IEEE Trans. Smart Grid*, vol. 5, no. 2, pp. 992–1001, Mar. 2014.

[16] A. Kuperman, U. Levy, J. Goren, A. Zafransky, and A. Savernin, "Battery charger for electric vehicle traction battery switch station," *IEEE Trans. Ind. Electron.,* vol. 60, no. 12, pp. 5391–5399, Dec. 2013.

[17] M. Lin *et al.*, "A new PWM strategy for grid-connected half-bridge active NPC converters with losses distribution balancing mechanism," *IEEE Trans. Power Electron.*, vol. 30, no. 9, pp. 5331–5340, Sep. 2015.

[18] A. Javadi, A. Hamadi, M. Haddad, S. Rahmani, and K. Al-Haddad, "A novel hybrid detection approach for series compensation under grid perturbation," in *Proc. IEEE Int. Conf. Ind. Technol. (ICIT),* Seville, Spain, 2015, pp. 2565–2570.
[19] E. Figueres, G. Garcera, J. Sandia, F. Gonzalez-Espin, and J. C. Rubio, "Sensitivity study of the dynamics of three-phase photovoltaic inverters with an LCL grid filter," *IEEE Trans. Ind. Electron.*, vol. 56, no. 3, pp. 706–717, Mar. 2009.
[20] A. Javadi, A. Hamadi, and K. Al-Haddad, "Stability analysis and effects of dampers on series active compensator," in *Proc. IEEE 23rd Int. Symp. Ind. Electron. (ISIE)*, Istanbul, Turkey, 2014, pp. 2173–2179.

Alireza Javadi (S'09) received the B.Sc. degree in power electrical engineering from the K. N. Toosi University of Technology, Tehran, in 2007, the M.Sc.A. degree in electrical engineering from the École Polytechnique de Montréal, Montreal, QC, Canada, in 2009, and the Ph.D. degree from the École de Technologie Supérieure (ÉTS), Montreal, in 2016. He is currently a Post-Doctoral Fellow with the NSERC-CRSNG, the Canada Research Chair with Electrical Energy Conversion and Power Electronics, ÉTS. His research interests encompass power electronics converters, harmonics, and reactive power control using hybrid active filters, power quality of smart grids, renewable energy, fast electric vehicle charging stations, real-time power hardware-in-the-loop applications, and rapid control prototyping.

He is an Active Member of the IEEE Montreal section and a Former President of the IEEE-ÉTS. He is a Registered Engineer with the Province of Quebec, Canada.

Abdelhamid Hamadi received the Bachelor of Engineering degree in power electronics from the University of Polytechnics, Ecole Nationale Polytechnique, Algiers, Algeria, in 1987, and the M.Sc. and Ph.D. degrees from the École de Technologie Supérieure, Montreal, QC, Canada, in 2004 and 2010, respectively, with theses entitled *Improved Performance of the Active Filter: Application of the Full Proportional Controller and Fuzzy Controller* and *Contribution to the Study of Hybrid Power Filters Used to Improve Power Quality in the Electrical Distribution Network*.

He is currently a Post-Doctoral Fellow with the Department of Electrical Engineering, École de Technologie Supérieure. His research interests include the application of power electronics in distribution systems, power quality analysis, active power filters, hybrid power filters, series hybrid filters, passive filters, and renewable energy.

Auguste Ndtoungou received the Ph.D. degree from the University of Paris XI, France, in 1996. From 1997, he has been a Professor with the Electrical Engineering, École Polytechnique de Masuku, Gabon. He is currently an Invited Professor with the Department of Electrical Engineering, École de Technologie Supérieure, Montreal, Canada. His research interests include power electronics, power quality, and renewable energy.

Kamal Al-Haddad (S'82-M'88-SM'92-F'07) received the B.Sc.A. and M.Sc.A. degrees from the University of Québec à Trois-Rivières, Canada, in 1982 and 1984, respectively, and the Ph.D. degree from the Institute National Polythechnique, Toulouse, France, in 1988. Since 1990, he has been a Professor with the Electrical Engineering Department, École de Technologie Supérieure, Montreal, QC, where he has been the holder of the Canada Research Chair in Electric Energy Conversion and Power Electronics since 2002. He has supervised over 100 Ph.D. and M.Sc.A. students working in the field of power electronics. He is a Consultant and has established very solid link with many Canadian industries working in the field of power electronics, electric transportation, aeronautics, and telecommunications. He has co-authored over 500 transactions and conference papers. His fields of interest are in high efficient static power converters, harmonics, and reactive power control using hybrid filters, switch mode, and resonant converters including the modeling, control, and development of prototypes for various industrial applications in electric traction, renewable energy, power supplies for drives, and telecommunication.

He was a recipient of the Dr.-Ing. Eugene Mittelmann Achievement Award. He is the President of the IEEE Industrial Electronics Society (IES) from 2016 to 2017, an Associate Editor of the IEEE TRANSACTIONS ON INDUSTRIAL INFORMATICS, and an IES Distinguished Lecturer. He is a Fellow Member of the Canadian Academy of Engineering.